

AperTO - Archivio Istituzionale Open Access dell'Università di Torino

**The interaction of H<sub>2</sub>O<sub>2</sub> with TiAlPO-5 molecular sieves: probing the catalytic potential of framework substituted Ti ions**

**This is the author's manuscript**

*Original Citation:*

*Availability:*

This version is available <http://hdl.handle.net/2318/138385> since

*Published version:*

DOI:10.1039/c3cp51214b

*Terms of use:*

Open Access

Anyone can freely access the full text of works made available as "Open Access". Works made available under a Creative Commons license can be used according to the terms and conditions of said license. Use of all other works requires consent of the right holder (author or publisher) if not exempted from copyright protection by the applicable law.

(Article begins on next page)



# UNIVERSITÀ DEGLI STUDI DI TORINO

5

***This is an author version of the contribution published on:***

*Questa è la versione dell'autore dell'opera:*

*[Phys. Chem. Chem. Phys., 15, 2013, 10.1039/c3cp51214b]*

10 *ovvero [Chiara Novara, Almudena Alfayate, Gloria Berlier, Sara Maurelli and Mario Chiesa, 15, RSC, 2013, 11099--11105]*

***The definitive version is available at:***

*La versione definitiva è disponibile alla URL:*

*[<http://pubs.rsc.org/en/journals/journalissues/cp#!recentarticles&all>]*

15

# The Interaction of H<sub>2</sub>O<sub>2</sub> with TiAlPO-5 Molecular Sieves. Probing the Catalytic Potential of Framework Substituted Ti Ions.

Chiara Novara,<sup>a</sup> Almudena Alfayate,<sup>b</sup> Gloria Berlier,<sup>a</sup> Sara Maurelli<sup>a</sup> and Mario Chiesa<sup>a\*</sup>

- 5 A combination of EPR, ENDOR and HYSORE experiments has been used to investigate the reactivity of hydrogen peroxide with TiAlPO-5 materials under both hydrated and anhydrous conditions. Superoxide radical anions, generated upon reaction, are used as paramagnetic probes to investigate the nature and reactivity of framework incorporated Ti ions. Super hyperfine interactions with <sup>27</sup>Al, <sup>31</sup>P and <sup>1</sup>H are resolved, which allow a detailed mapping of the local environment of the adsorbed O<sub>2</sub><sup>-</sup> ions.
- 10 Evidence is provided for the first time of a specific redox activity associated to Ti ions incorporated at framework Al sites of TiAlPO materials.

## Introduction

The incorporation of transition metal ions (TMIs) into the framework of microporous and mesoporous materials is a key strategy in the quest for new and efficient heterogeneous catalysts. As an example, isomorphous substitution of Ti in the lattice of zeotype materials, 15 e.g., TS-1 zeolites, results in active catalysts for the liquid-phase catalytic oxidation of a variety of organic compounds with H<sub>2</sub>O<sub>2</sub>.<sup>1</sup> Analogously, Ti(IV) ions can also be incorporated through isomorphous substitution of tetrahedrally-coordinated elements (T-sites) in the strictly alternating [PO<sub>4</sub>]<sup>3-</sup> and [AlO<sub>4</sub>]<sup>5-</sup> tetrahedra of the so-called crystalline, microporous AlPO<sub>4</sub> materials. A large body of work has been done concerning the spectroscopic characterization of oxygen intermediates in the case of H<sub>2</sub>O<sub>2</sub>-treated TS-1.<sup>2-6</sup> Comparatively, much less data are available for the same process occurring on Ti-AlPO materials, which have proved to be effective catalysts in the 20 oxidation of olefins using H<sub>2</sub>O<sub>2</sub>.<sup>7</sup>

Most studies concerning oxidation reactions with Ti-containing materials are dealing with aqueous H<sub>2</sub>O<sub>2</sub> (HP) as oxidant. It is known that the presence of protic solvents such as water affects the catalytic pathway of reaction leading to equilibria between different intermediates.<sup>8,9</sup>

This problem can be circumvented using an anhydrous source of hydrogen peroxide such as KH<sub>2</sub>PO<sub>4</sub>-H<sub>2</sub>O<sub>2</sub> adducts<sup>8</sup> or anhydrous 25 crystalline urea adducts of hydrogen peroxide (UHP)<sup>9</sup> which slowly release anhydrous H<sub>2</sub>O<sub>2</sub> by thermal decomposition. UHP has been successfully employed for the epoxidation of substituted allylic alcohols<sup>9</sup> and styrene,<sup>10,11</sup> in the presence of TS-1 as redox catalyst, producing excellent epoxide yields. Since UHP releases anhydrous H<sub>2</sub>O<sub>2</sub>, it has provided interesting information on the nature of the active sites in TS-1 and TS-2.<sup>12</sup>

In all cases the interaction of H<sub>2</sub>O<sub>2</sub> (both hydrated and anhydrous) with Ti containing catalysts leads to the formation of O<sub>2</sub><sup>-</sup> species. Ti- 30 superoxo species have been identified as active centers in styrene<sup>10,11</sup> and propane<sup>13</sup> oxidations over TS-1. Moreover, the superoxide ion, besides having an intrinsic interest as a potentially active catalytic species, constitutes a particularly useful paramagnetic probe for monitoring the local environment of the active Ti site when EPR spectroscopy is used.<sup>14</sup>

Spectroscopic techniques capable of selectively probing the active sites, even though they constitute only a minor fraction of the total amount of TMI sites, are of fundamental importance in providing detailed mechanistic insights and assist in the design and development 35 of novel selective oxidation catalysts.<sup>15</sup> Advanced EPR methods, in particular hyperfine techniques (HYSORE and ENDOR) provide invaluable information about both structural and chemical aspects of the catalytically active paramagnetic centers, such as their geometry, localization and electronic structure, which ultimately governs their chemical reactivity and their catalytic potential.

We recently reported a series of papers<sup>16-18</sup> devoted to the detailed spectroscopic characterization of the active sites of TiAlPO-5 systems using a combination of advanced EPR methods and DRUV-Vis spectroscopy to monitor the nature of reduced titanium species. 40 In particular we focused on reduced Ti<sup>3+</sup> species and their coordinating chemistry, providing firm evidence for Ti incorporation into the AlPO<sub>4</sub> frame-work at Al<sup>3+</sup> sites and demonstrating the existence of Ti-O-Ti pairs whereby two titanium ions substitute a Al<sup>3+</sup>/P<sup>5+</sup> pair. The intriguing fact, emerging from these studies and unique to the AlPO<sub>4</sub> system, is that Ti ions substituting Al<sup>3+</sup> cations are active redox centers (Ti<sup>4+</sup>/Ti<sup>3+</sup>) while Ti ions at P sites (where P has a formal +5 charge) are much harder to reduce, but can act as coordinating centers because of its unsaturated nature. With this in mind in the present work we investigate the interaction of a TiAlPO-5 catalyst with 45 both aqueous and anhydrous H<sub>2</sub>O<sub>2</sub> monitoring the formed Ti-superoxo species by means of continuous wave (CW) EPR and hyperfine techniques. The results are compared to Ti-superoxide species formed by direct oxidation of the reduced sample with molecular oxygen, leading to detailed understanding of structure-property correlations and mechanistic implications at the basis of the catalytic potential of these materials.

## Experimental Section

### 50 Sample preparation

Experiments were performed on TiAlPO-5 materials obtained by hydrothermal synthesis following the procedure described in the literature.<sup>19,20</sup>

A proper amount of aluminum oxide hydroxide (Catapal B Alumina, Sasol) was added to distilled water and stirred vigorously before adding titanium isopropoxide (Aldrich), phosphoric acid (Sigma-Aldrich) and triethylamine (TEA, Sigma-Aldrich), resulting in a gel composition 0.1 TiO<sub>2</sub>: 1 TEA: 1 Al<sub>2</sub>O<sub>3</sub>: 1 P<sub>2</sub>O<sub>5</sub>: 40 H<sub>2</sub>O. The gel was transferred to a Teflon lined stainless steel autoclave and kept at autogeneous pressure at 175° C for 24 hours. After this, the autoclave was cooled to room temperature and the solid product was washed several times with distilled water, filtered and dried in an air oven at 110° C for 12 hours. Finally the product was calcined by heating until 550° C in a flow of nitrogen and kept at the same temperature in oxygen for 12 hours. The calcined sample is white in color and EPR silent.

10 Prior to further treatments, calcined samples were dehydrated under vacuum by gradually raising the temperature to 423 K over a period of 1 hour in order to remove the physisorbed water.

### Reaction with H<sub>2</sub>O<sub>2</sub> and UHP

The reactions of TiAlPO-5 with aqueous H<sub>2</sub>O<sub>2</sub> (30%, Fluka TraceSELECT) and anhydrous H<sub>2</sub>O<sub>2</sub> developed by the thermal decomposition of crystalline H<sub>2</sub>O<sub>2</sub> – Urea adduct (UHP, Fluka) were performed at room temperature directly in the cell used for the 15 spectroscopic characterization.

The calcined TiAlPO-5 has been impregnated with H<sub>2</sub>O<sub>2</sub> for 2 hours and subsequently dried in air at room temperature, resulting in a yellow powder. The sample was then gradually evacuated at room temperature for 24 hours. A white powder was obtained at the end of this treatment.

20 To compel its thermal decomposition, the UHP powder (previously outgassed in a glass ampoule) was warmed up to 328 K and the developed H<sub>2</sub>O<sub>2</sub> sent through the vacuum line to the cell containing the calcined TiAlPO-5 sample, previously oxidized and outgassed. The required reaction time was 2 hours.

### Spectroscopic measurements

For the spectroscopic characterization of all the samples a quartz tubular cell allowing in situ EPR measurements has been employed.

25 *X-band CW EPR* spectra were detected at 77 K on a Bruker EMX spectrometer (microwave frequency 9.75 GHz) equipped with a cylindrical cavity. A microwave power of 1 mW, modulation amplitude of 0.1 mT and a modulation frequency of 100 kHz were used. Pulse EPR experiments were performed on an ELEXYS 580 Bruker spectrometer (at the microwave frequency of 9.76 GHz) equipped with a liquid-helium cryostat from Oxford Inc. All experiments were performed at 10 K unless elsewhere stated. The magnetic field was measured by means of a Bruker ER035M NMR gaussmeter.

30 *Electron-spin-echo (ESE)* detected EPR experiments were carried out with the pulse sequence:  $\pi/2 - \tau - \pi - \tau - echo$ , with microwave pulse lengths  $t_{\pi/2} = 16$  ns and  $t_{\pi} = 32$  ns and a  $\tau$  value of 200 ns.

Mims ENDOR spectra were measured with the mw pulse sequence  $\pi/2 - \tau - \pi/2 - T - \pi/2 - \tau - echo$  with  $t_{\pi/2} = 16$  ns. In order to remove blind spots effects time  $\tau$  was increased in steps of 16 ns from 96 ns to 576 ns and the spectra were added together. During the time  $T$  a radio frequency pulse was applied, the length of which has been optimized for the two different nuclei (<sup>31</sup>P and <sup>1</sup>H) by a nutation experiment. Optimal lengths were found to be 10.5  $\mu$ s and 12  $\mu$ s for <sup>31</sup>P and <sup>1</sup>H respectively.

35 *Matched HYSORE experiments*<sup>21</sup> have been performed with the sequence  $\pi/2 - \tau - (HTA) - t_1 - \pi - t_2 - (HTA) - \tau - echo$  with mw pulse length  $t_{\pi/2} = 16$  ns and  $t_{\pi} = 16$  ns. The amplitude of the microwave field of the matching pulses was 15.6 MHz. The optimal length of the high turning angle (HTA) pulse was experimentally determined with a 2D three-pulse experiment where the pulse length of the second and third pulses were increased in steps of 8 ns starting from 16 ns. The optimal value was found to be 80 ns.

40 The time traces of the HYSORE spectra were baseline corrected with a third-order polynomial, apodized with a Hamming window and zero filled. After two-dimensional Fourier transformation, the absolute value spectra were calculated. The spectra were added for the different  $\tau$  values, that are detailed in the figure captions, in order to eliminate blind-spot effects.

The Mims-ENDOR and HYSORE spectra were simulated using the Easyspin Matlab package.<sup>22</sup>

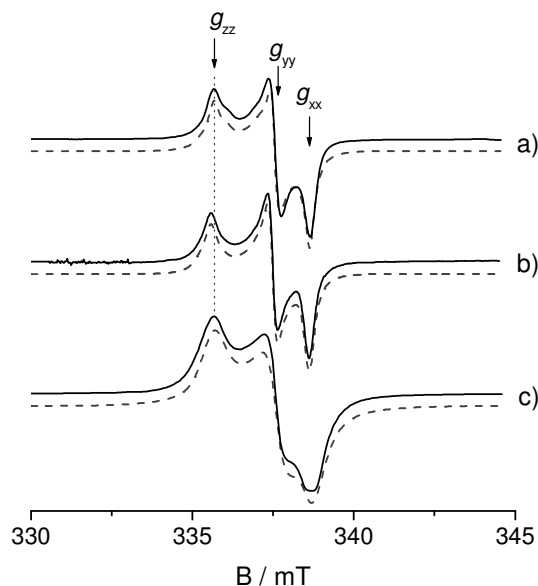
## Results and Discussion

45 Conventional characterization of the TiAlPO-5 materials by means of powder X-ray diffraction and scanning electron microscopy, either before or after calcination, indicated that the samples are exclusively formed by a crystalline AFI-structured phase.

When TiAlPO-5 was stirred with aqueous H<sub>2</sub>O<sub>2</sub> (30 wt% H<sub>2</sub>O<sub>2</sub>) for about 2 hours at room temperature, and subsequently gently dried in air at the same temperature, the sample became yellow. Associated to this color, weak and poorly resolved EPR spectra (not shown), characterized by a rhombic powder pattern with a broad and ill-defined  $g_{zz}$  peak at  $\approx 2.02$  were observed, in agreement with previous reports.<sup>23</sup> DR UV-Vis spectra (Supporting Information) show characteristic absorption bands at 260 and 380 nm. The latter is very 50 similar to that reported for TS-1 measured under similar conditions, and can be assigned to side-on  $\eta^2$ -peroxo complexes.<sup>24</sup> The yellow sample was subsequently evacuated to a residual pressure of about 10<sup>-4</sup> mbar. Upon this dehydrating treatment a decrease in intensity of the absorption band at 380 nm is observed. The same behavior has been reported in the case of TS-1 and explained in terms of the conversion of  $\eta^2$ -side on peroxo complexes into end-on  $\eta^1$ -hydroperoxo species.<sup>24</sup> Accompanied to the fading of the yellow color, a large increase in the EPR spectral intensity is observed. A typical EPR spectrum for this evacuated sample is shown in Figure 1a. The 55 spectrum is dominated by a well defined orthorhombic signal, typical of an O<sub>2</sub><sup>-</sup> type species, with  $g$  values of  $g_{zz} = 2.0212$ ,  $g_{yy} = 2.0098$

and  $g_{xx} = 2.0033$ . A second less abundant species characterized by a lower  $g_{zz}$  value of 2.019 is also present.

A similar spectrum to the one previously described is obtained upon reaction of the TiAlPO-5 sample with anhydrous  $H_2O_2$  generated by thermal decomposition of UHP. The EPR spectrum recorded at 77 K is shown in Figure 1b. Inspection of the spectrum reveals small differences with respect to the one obtained by reaction with aqueous  $H_2O_2$ . In particular the  $g_{zz}$  component of the dominant species is slightly shifted towards lower field ( $g_{zz} = 2.0215$ ) and displays a slightly broader line width. We remark that this case is different from what reported by Kumar and co-workers<sup>12</sup> in the case of the same reaction carried out using titanium silicalite (TS-1 and TS-2). In that case the use of anhydrous  $H_2O_2$  led to an EPR spectrum characterized by a high level of heterogeneity, indicating a number of different Ti sites. Such a speciation is not observed in the case of the TiAlPO-5 sample.



**10** **Figure 1.** Experimental (solid lines) and simulated (dotted lines) CW-EPR spectra of  $O_2^-$  radical ions on TiAlPO-5 obtained by reaction with a) hydrated  $H_2O_2$ , b) anhydrous  $H_2O_2$  (from UHP) and c) oxidation of the reduced TiAlPO-5 with molecular  $O_2$ . All spectra are recorded at 77 K. The spin Hamiltonian parameters extracted from the simulations are listed in Table 1.

For the sake of comparison, in Figure 1c we also report the EPR spectrum of the superoxide radical anion obtained by reaction of molecular oxygen with a reduced TiAlPO-5 sample. In this case  $Ti^{3+}$  centers were generated upon reduction of the sample with molecular hydrogen as detailed elsewhere.<sup>16</sup> The so formed  $Ti^{3+}$  species react with oxygen via a one-electron transfer mechanism leading to side-on superoxide radical anions adsorbed on the surface.<sup>17</sup> The resulting  $O_2^-$  displays a significantly higher intensity and correspondingly broader line widths, with respect to the previous cases. Interestingly the  $g_{zz}$  component of this signal ( $g_{zz} = 2.0212$ ) is the same as that of the  $O_2^-$  obtained by reaction with aqueous hydrogen peroxide. The spin Hamiltonian parameters for the three different superoxides, as obtained by computer simulation of the EPR spectra, are listed in Table 1.

**20** The fact that in all cases we only observe nearly a single site for the  $O_2^-$  adsorption, seems to indicate that on TiAlPO-5 the site heterogeneity is limited and/or that the chemical reactivity is driven by isolated specific sites with well defined characteristics. Also, the small differences in the  $g$  values between the superoxide radicals generated by reaction with aqueous and anhydrous  $H_2O_2$  suggest small differences in the local environments of the  $O_2^-$  in the two cases. In order to clarify the origin of these differences and to further investigate the details of the active sites and their chemical activity, ENDOR and HYSORE experiments have been performed on the **25** different systems.

ENDOR spectra were recorded at three different magnetic field settings, corresponding to the  $O_2^-$  principal  $g$  values of the EPR spectra previously described. The spectra recorded at a field position corresponding to the  $O_2^-$   $g_{xx}$  component are shown in Figure 2 (spectra recorded at other magnetic field settings are shown as Supporting Information).

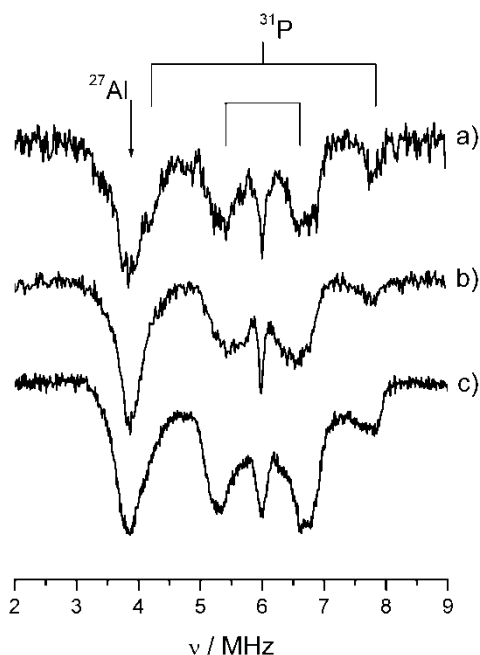


**Figure 2.** Mims ENDOR spectra of  $O_2^-$  radical anions adsorbed on TiAlPO-5 generated by a) reaction of the oxidized sample with hydrated  $H_2O_2$ ; b) reaction with anhydrous  $H_2O_2$  (from UHP); c) oxidation with molecular  $O_2$  of the reduced sample. All spectra were recorded at 10K at field position corresponding to the  $O_2^-$   $g_{xx}$  component.

5 For all spectra, the ENDOR powder pattern consists of a series of symmetric transitions with respect to the  $^{27}Al$ ,  $^{31}P$  and  $^1H$  nuclear Larmor frequencies ( $\nu_{Al} \approx 3.88$  MHz,  $\nu_P \approx 5.97$  MHz,  $\nu_H \approx 14.9$  MHz) having the characteristic shape of a powder pattern due to an axially symmetric tensor. The feature centered at about 4 MHz is due to the contribution of remote  $Al^{3+}$  ions and overlaps with the lowest  $^{31}P$  parallel component.

Sample	$g_x$ $\pm 0.0003$	$g_y$ $\pm 0.0003$	$g_z$ $\pm 0.0003$	$(^1H) a_{iso}$ $\pm 0.1$	$(^1H) T$ $\pm 0.5$	$\beta$ $\pm 20$	$(^{31}P) a_{iso}$ $\pm 0.1$	$(^{31}P) T$ $\pm 0.5$	$\beta$ $\pm 10$	Ref.
Aqueous $H_2O_2$	2.0033	2.0098	2.0212	-0.13	2.0	70	0.23	1.88	80	This work
UHP	2.0032	2.0100	2.0215	+2.0	5.5	70	0.23	1.88	80	This work
TiAlPO-5 + $O_2$	2.0034	2.0099	2.0212	-0.13	2.0	70	0.23	1.88	80	17

10 **Table 1.** Spin-Hamiltonian parameters for  $O_2^-$  radical anions generated on TiAlPO-5 upon different treatments. The parameters are derived from the computer simulations of the experimental spectra reported in Figure 1, Figure 3 and Supporting Information. Hyperfine couplings are given in MHz, while Euler angles in degrees. Only the  $\beta$  angle is determined from the experiments.

The relatively large  $^{31}P$  hyperfine coupling and the negligible  $^{27}Al$  coupling unambiguously indicate that the superoxide radical anion (consistently with the observed  $g_z$  factor) is stabilized on  $Ti^{4+}$  ions substituting the framework  $Al^{3+}$ . This situation holds for the three different cases, thus regardless to the chemical pathway followed in the generation of the superoxide anion, this is stabilized on the same site, showing that the reactivity of the system is intimately linked to the  $Ti^{4+}/Ti^{3+}$  redox activity of Ti ions at  $Al^{3+}$  sites, in good agreement with previous evidences.<sup>16,17</sup>

15 While the  $^{31}P$  hyperfine interactions do not change for the three different systems, the  $^1H$  hyperfine interaction depends on the generation method. In particular a distinct difference is observed in the maximum proton coupling for the  $O_2^-$  generated via reaction of the sample with anhydrous  $H_2O_2$  ( $\approx 10$  MHz) and 30% aqueous solution  $H_2O_2$  ( $\approx 3.5$  MHz). Interestingly, this latter value is analogous to 20 that observed upon oxidation of the reduced sample with molecular  $O_2$ .

The  $^1H$  ENDOR spectra were relatively weak and poorly resolved. A better resolution was obtained by means of  $^1H$  matched HYSCORE experiments. The  $^1H$  matched HYSCORE spectra recorded at a magnetic field setting corresponding to the  $g_{xx}$  component for the three different superoxide are shown in Figure 3(A).

25 Inspection of the figure shows that in the cases of  $O_2^-$  ions generated by reaction with hydrated  $H_2O_2$  and oxidation with  $O_2$ , the maximum  $^1H$  coupling is of the order of approximately 3.5 MHz (Figure 3 (a) and (c)). A much larger coupling of the order of 10 MHz is observed in the case of reaction with UHP (Figure 3 (b)). The full hyperfine tensor can be estimated by simulation of the HYSCORE spectra taken at different field positions (Figure 3(B)). The results of the simulation analysis are reported in Table 1. Assuming the sign of  $T$  as positive ( $g_n$  for H is positive) and representing the principal values of the dipolar tensor as  $[-T -T 2T]$ , with  $T$  defined as:

$$T = \frac{\mu_0}{4\pi} g_e g_n \beta_e \beta_n \frac{1}{r^3} \quad (1)$$

the values of  $a_{\text{iso}} = 2.0$  MHz and  $T = 5.5$  MHz were obtained.

Assuming that the anisotropic part of the hyperfine interaction is described as a purely point-dipolar interaction, the distance between the proton and the  $\text{O}_2^-$  radical anion can be estimated from Equation 1, to be of the order of 0.24 nm, clearly calling for a proton localized on a first neighbor framework oxygen. The presence of this proton may well justify the slight difference between the  $g_{zz}$  factors of the corresponding CW-EPR spectra (Figure 1a and 1b). This distance may be compared to the one associated to the weakly coupled proton observed in the case of reaction with aqueous  $\text{H}_2\text{O}_2$  of the order of 0.34 nm ( $T = 2.0$  MHz), which is only compatible with a proton stabilized on a non nearest neighbor oxygen. This is in total analogy with the case of  $\text{O}_2^-$  generated by reaction of molecular oxygen and discussed in ref 17. In all cases the hyperfine tensor structure and its orientation point to a T shaped structure of isocetes symmetry, which is consistent with the tetrahedral symmetry of the binding site.

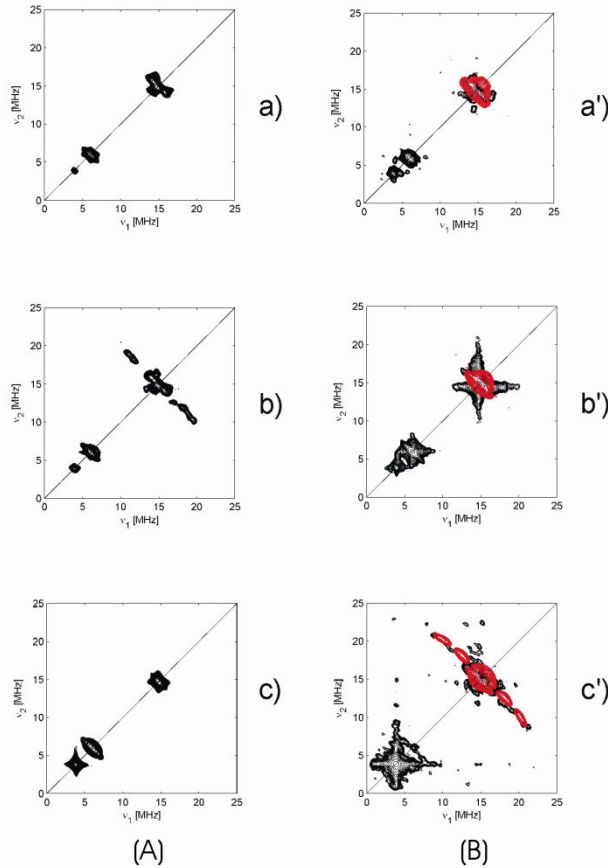


**Figure 3.** (A) Experimental  $^1\text{H}$  Matched HYSCORE spectra of  $\text{O}_2^-$  on TiAlPO-5, generated by a) reaction of the oxidized sample with hydrated  $\text{H}_2\text{O}_2$ ; b) reaction with anhydrous  $\text{H}_2\text{O}_2$  (from UHP); c) oxidation with molecular  $\text{O}_2$  of the reduced sample. All spectra are recorded at a magnetic field setting corresponding to the  $g_{xx}$  component of the EPR spectrum ( $B_0=348.3$  mT). (B) Experimental (black lines) and computer simulations (red lines) of  $^1\text{H}$  Matched HYSCORE spectra of TiAlPO-5 reacted with anhydrous  $\text{H}_2\text{O}_2$  (UHP) recorded at different magnetic field settings corresponding to a')  $g_{zz}$  component ( $B_0= 345.2$  mT); b')  $g_{yy}$  component ( $B_0=347.2$  mT) and c')  $g_{xx}$  component ( $B_0=348.3$  mT). Experimental and simulated HYSCORE spectra taken at two  $\tau$  values, (96 ns and 240 ns), were added together after Fourier transform.

The scenario emerging from the ENDOR and HYSCORE experiments can thus be summarized as follows. Upon contact with  $\text{H}_2\text{O}_2$  superoxide anions are formed and stabilized at framework Ti ions replacing  $\text{Al}^{3+}$  cations. Moreover, when UHP is used instead of hydrated  $\text{H}_2\text{O}_2$ , the presence of a residual  $\text{H}^+$  on an oxygen framework in the first coordination shell is observed.

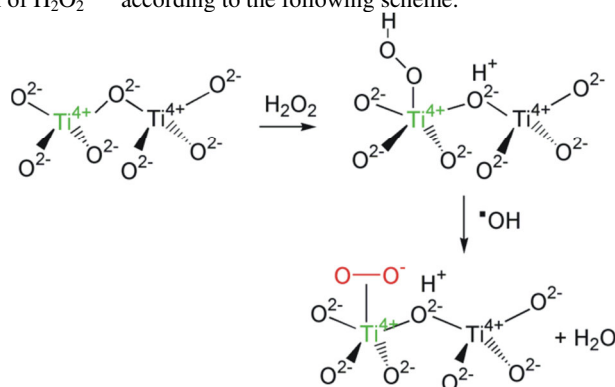
These observations together with previous findings reported by some of us<sup>16,17</sup> allow proposing a mechanistic pathway for this reaction, casting the role of Ti ions localized at  $\text{Al}^{3+}$  sites as prominent actors in the redox activity of TiAlPO materials. It seems natural to associate the redox activity of this specific Ti ion with the fact that the  $\text{Ti}^{3+}$  reduced state has the natural formal charge for this specific site. On the contrary Ti ions substituting a formally  $\text{P}^{5+}$  ion remain in the  $\text{Ti}^{4+}$  oxidation state (EPR silent) due to the large charge imbalance that would require two extra protons to compensate the extra charge. This picture is clearly the result emerging from the oxidation of the reduced TiAlPO-5 system. As already reported by some of us<sup>17</sup>, the observation of the  $^1\text{H}$  hyperfine interaction of about 3 MHz clearly proves that Ti-O-Ti pairs are formed as the corresponding  $\text{O}_2^-$ -H distance of about 0.34 nm is only compatible with a second Ti ion, substituting a  $\text{P}^{5+}$  ion at a next neighbor position forming a Ti-O-Ti oligomer.

When the sample reacts with  $\text{H}_2\text{O}_2$  the following equation may be written:



The conversion of peroxide to superoxide is a one-electron redox reaction and requires the presence of transition metals having accessible multiple oxidation states. Therefore, this reaction can help in elucidating the nature of redox active sites in the TiAlPO-5 system.

- 5 It is generally accepted that the first step in the oxidation by the TS-1/ $\text{H}_2\text{O}_2$  system is the formation of the  $\text{TiOOH}$  species, the species responsible for the epoxidation.<sup>25</sup>  $\text{TiOOH}$  can in turn be regarded as the precursor of the Ti-superoxo species via reaction with OH radicals generated by decomposition of  $\text{H}_2\text{O}_2$  [26] according to the following scheme:

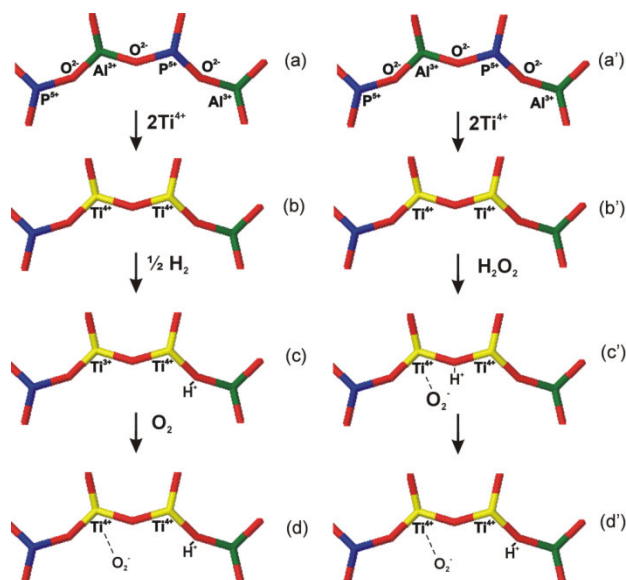


**Scheme 1.** Reaction pattern leading to  $\text{O}_2^-$  species. The Ti ion at the Al position is evidenced in green. The EPR active  $\text{O}_2^-$  species is in red.

- 10 Interestingly, both reactions (direct oxidation of the reduced sample and reaction with  $\text{H}_2\text{O}_2$  of the oxidized sample) lead to the stabilization of the superoxide radical anion on the same site (namely the  $\text{Ti}^{4+}$  ion occupying  $\text{Al}^{3+}$  position). Moreover a clear difference in the localization of the  $^1\text{H}$  moiety depending on the presence of the solvent is evidenced via hyperfine techniques. The presence of the solvent is clearly important in determining the reaction pathway. We recall that for TiAlPO-5 previously reacted with hydrated  $\text{H}_2\text{O}_2$ , out-gassing of the sample (which implies the practical water removal due to its lower vapor pressure) leads to a drastic increase of the  $\text{O}_2^-$  signal intensity. In the same context equilibria controlled by the degree of hydration between end-on hydroperoxo and side-on peroxy species have been reported by Bordiga et al.<sup>3</sup>

- 15 What seems clear is that in TiAlPO-5 Ti ions substituting  $\text{Al}^{3+}$  ions possess a higher redox reactivity (higher catalytic potential) with respect to Ti ions at P(V) sites. The observation of the large  $^1\text{H}$  hyperfine interaction upon reaction with anhydrous  $\text{H}_2\text{O}_2$  reveals that the reaction takes place over this Ti center resulting in the stabilization of the  $\text{O}_2^-$  and of a proton in a first neighboring oxygen as represented in Scheme 1. Simple electrostatic arguments suggest however that this situation is relatively unstable due to the overall charge imbalance at the Ti ion replacing an  $\text{Al}^{3+}$  cation. We already demonstrated that the incorporation mechanism of Ti in the AlPO-5 structure involves the substitution of a  $\text{Al}^{3+}/\text{P}^{5+}$  couple by two  $\text{Ti}^{4+}$  ions (Scheme 2b'). The key point to be stressed is that these two Ti ions are not equivalent from the point of view of reactivity. In fact the Ti ion replacing for the  $\text{Al}^{3+}$  has redox capability and can be reduced to  $\text{Ti}^{3+}$  (Scheme 2c) or undergo a one electron transfer reaction to form the  $\text{O}_2^-$  radical (Scheme 2c'). Notice that in both cases the overall charge at this site is +3 (corresponding to that of the original  $\text{Al}^{3+}$ ) and a compensating positive charge is now needed close to the Ti ion substituting for the  $\text{P}^{5+}$  to keep the charge balance. The proton charge in c' will be actually "shared" between the two Ti ions creating a charge imbalance at the Ti ion replacing for  $\text{Al}^{3+}$ . We therefore argue that a more energetically stable situation is reached if the proton migrates away from the oxygen atom contiguous to the Ti at the Al site to an oxygen linked to the  $\text{Ti}^{4+}$  at the  $\text{P}^{5+}$  site. This is actually the situation monitored upon reaction with aqueous  $\text{H}_2\text{O}_2$ . It may be argued that the presence of the water molecules favors the migration of the  $\text{H}^+$  species via hydrogen bond network. Also it should be considered that the spectra are recorded upon out-gassing of the sample at room temperature so that during this process the metastable situation where the  $\text{H}^+$  is stabilized at the reaction site evolves towards a more deep energy minimum. This minimum is represented by an  $\text{O}_2^-$  adsorbed on a Ti(IV) at a pristine Al(III) site and a proton stabilized nearby a Ti(IV) at a P(V) site. This situation is also detected by the reaction of molecular oxygen with the reduced TiAlPO-5 sample and provides compelling evidence for the existence of Ti-O-Ti units in the system, emphasizing the role of Ti ions at Al sites as a species with the highest redox potential. This situation is summarized in Scheme 2 where the reaction pathway for the formation of side-on  $\text{O}_2^-$  species under the different conditions considered is shown.





**Scheme 2.**  $\text{O}_2^-$  formation mechanisms. See text for explanation.

## Conclusions

5 We have investigated by means of advanced EPR techniques the reactivity of hydrogen peroxide under both hydrated and anhydrous conditions with TiAlPO-5 materials. The formed superoxide radical anions have been used as paramagnetic probes to monitor the characteristics of the reactive site under the different reaction conditions. The peculiar reactivity of Ti ions substituted at framework Al sites is evidenced providing the first relevant indication of a specific redox activity associated to this particular site. These results bring into prominence the importance of the chemical nature of the framework in driving the chemical reactivity and catalytic potential of substituted TMIs. We expect that these results will be of importance in the context of designing efficient catalysts with specific functionalities tailored upon specific and selective reactions.

## Acknowledgements

A.A. acknowledges CSIC for a PhD JAE-predoc fellowship and for financing her stay in Torino.

## 15 Notes and references

[a] Ms. C. Novara, Dr. G. Berlier, Dr. S. Maurelli, Prof. M. Chiesa  
 Dipartimento di Chimica, Università degli Studi di Torino, Via Giuria, 7 10125-Torino, Italy  
 Fax: (+) 390116707855  
 E-mail: mario.chiesa@unito.it

20 [b] Ms. A. Alfayate Instituto de Catálisis y Petroleoquímica, ICP-CSIC  
 C/ Marie Curie 2, 28049 Madrid, Spain

† Electronic Supplementary Information (ESI) available: [UV-Vis spectra, experimental and simulated ENDOR spectra at different magnetic field settings].

- 25
- 1 B. Notari, in *Studies in Surface Science and Catalysis* (Eds.: P. J. Grobet, W. J. Mortier, E. F. Vansant, G. Schulz-Ekloff), Elsevier, Amsterdam, 1988, **37**, 413; M. G. Clerici and U. Romano, Eur. Patent EP100119A1, 1983; G. Bellusi, A. Giusti, A. Esposito and F. Buonomo, Eur. Patent EP226257A2, 1987; B. Notari, *Adv. Catal.*, 1996, **41**, 253.
  - 30 2 I. W. C. E. Arends, R. A. Sheldon, M. Wallau and U. Schuchardt, *Angew Chemie Int. Ed. Engl.*, 1997, **36**, 1144; G. Bellussi, A. Carati, M. G. Clerici, G. Maddinelli and R. Millini, *J. Catal.*, 1992, **133**, 220; S. Gontier and A. Tuel, *J. Catal.*, 1995, **157**, 124; E. Duprey, P. Beaudier, M. A. Springuel-Huet, F. Bozon-Verduraz, J. Fraissard, J. M. Manoli and J. M. Bregeault, *J. Catal.*, 1997, **165**, 22; W. Y. Lin and H. Frei, *J. Am. Chem. Soc.*, 2002, **124**, 9292; C. B. Khouw, C. B. Dartt, J. A. Labinger and M. E. Davis, *J. Catal.*, 1994, **149**, 195.
  - 3 S. Bordiga, F. Bonino, A. Damin and C. Lamberti, *Phys. Chem. Chem. Phys.*, 2007, **9**, 4854.
  - 35 4 G. Tozzola, M. A. Mantegazza, G. Ranghino, G. Petrini, S. Bordiga, G. Ricchiardi, C. Lamberti, R. Zulian and A. Zecchina, *J. Catal.*, 1998, **179**, 64.
  - 5 G. Ricchiardi, A. Damin, S. Bordiga, C. Lamberti, G. Spano, F. Rivetti and A. Zecchina, *J. Am. Chem. Soc.*, 2001, **123**, 11409.
  - 6 C. Lamberti, S. Bordiga, A. Zecchina, G. Artioli, G. Marra and G. Spano, *J. Am. Chem. Soc.*, 2001, **123**, 2204.
  - 7 S.-O. Lee, R. Raja, K. D. M. Harris, J. M. Thomas, B. F. G. Johnson, and G. Sankar, *Angew. Chem. Int. Ed.*, 2003, **42**, 1520.

- 8 C. Prestipino, F. Bonino, A. Usseglio Nanot, A. Damin, A. Tasso, M. G. Clerici, S. Bordiga, F. D'Acapito, A. Zecchina and C. Lamberti, *ChemPhysChem*, 2004, **5**, 1799.
- 9 W. Adam, R. Kumar, T. I. Reddy and M. Renz, *Angew. Chem. Int. Ed.*, 1996, **35**, 880.
- 10 J. Q. Zhuang, G. Yang, D. Ma, X. J. Lan, X. M. Liu, X. W. Han, X. H. Bao and U. Mueller, *Angew. Chem. Int. Ed.*, 2004, **43**, 6377.
- 5 11 S. C. Laha and R. Kumar, *J. Catal.*, 2001, **204**, 64.
- 12 S. C. Laha and R. Kumar, *J. Catal.*, 2002, **208**, 339.
- 13 S. Heinrich, M. Plettig and E. Klemm, *Catal. Lett.*, 2011, **141**, 251.
- 14 M. Anpo, M. Che, B. Fubini, E. Garrone, E. Giamello and M. C. Paganini, *Top. Catal.*, 1999, **8**, 189.
- 15 R. M. Leithall, V. N. Shetti, S. Maurelli, M. Chiesa, E. Gianotti and R. Raja, *J. Am. Chem. Soc.*, 2013, DOI: 10.1021/ja3119064
- 10 16 S. Maurelli, V. Muthusamy, M. Chiesa, G. Berlier and S. Van Doorslaer, *J. Am. Chem. Soc.*, 2011, **133**, 7340.
- 17 S. Maurelli, M. Vishnuvarthan, G. Berlier and M. Chiesa, *Phys. Chem. Chem. Phys.*, 2012, **14**, 987.
- 18 S. Maurelli, M. Chiesa, E. Giamello, R. M. Leithall and R. Raja, *Chem. Commun.*, 2012, **48**, 8700.
- 19 E. M. Flanigen, B. M. T. Lok, R. L. Patton and S. T. Wilson, US Patent 4759919, 1988.
- 20 S. P. Elangovan and V. Murugesan, *J. Mol. Catal. A - Chem.*, 1997, **118**, 301.
- 15 21 G. Jeschke, R. Rakhmatullin and A. Schweiger, *J. Magn. Reson.*, 1998, **131**, 261.
- 22 S. Stoll and A. Schweiger, *J. Magn. Reson.*, 2006, **42**, 55.
- 23 K. L. Antcliff, D.M. Murphy, E. Griffiths and E. Giamello, *Phys. Chem. Chem. Phys.*, 2003, **5**, 4306.
- 24 F. Bonino, A. Damin, G. Ricchiardi, M. Ricci, G. Spanò, R. D'Aloisio, A. Zecchina, C. Lamberti, C. Prestipino, S. Bordiga *J. Phys. Chem B*, 2004, **108**, 3573.
- 20 25 M. G. Clerici and P. Ingallina, *J. Catal.*, 1993, **140**, 71; S. Bordiga, A. Damin, F. Bonino, G. Ricchiardi, C. Lamberti and A. Zecchina, *Angew. Chem. Int. Ed.*, 2002, **41**, 4734.
- 26 F. Geobaldo, S. Bordiga, A. Zecchina, E. Giamello, G. Leofanti and G. Petrini, *Catal. Lett.*, 1992, **16**, 109..